Theory of the capping effect in magnetic double-film systems

Xiao Hu and Yoshiyuki Kawazoe
Institute for Materials Research, Tohoku University, 2-1-1 Katahira, Aoba-ku, Sendai 980, Japan
(Received 10 June 1993; revised manuscript received 12 October 1993)

The capping effect in magnetic double-film systems has been studied theoretically by means of a variational method for magnetic energies in a continuum model. The coercive force of the double-film system is given explicitly in terms of the magnetic constants of the two films. A field $H_{\rm cap}$ is defined regarding the exchange coupling between the films as an effective Zeeman energy, and it is found that $H_{\rm cap}$ enhances the external field in recording processes. Since $H_{\rm cap}$ felt by the magnetization in the recording film is localized near the interface, a domino phenomenon of magnetization in the recording film is expected. It is triggered by accidental nucleations at the interface, as part of the dynamic process of recording. A phase transition between different alignments of magnetization is found when the thickness of the capping film is varied and the mechanism of this phase transition is clarified. The critical point is derived analytically which gives also the minimal thickness of the capping film that shows the capping effect. It is found that the critical behavior of $H_{\rm cap}$ in the vicinity of the minimal thickness is characterized by an exponent $\beta=1$. The capping effect at large thickness limit is also discussed.

I. INTRODUCTION

Magnetic multifilm systems have attracted much attention recently, because of the development of technologies which can control the growth of ultrathin films. Many fundamental physical phenomena have been discovered in multifilm systems, and these systems have potential applications such as recording media and recording devices. Many ingenious and useful implementations have been developed for magneto-optic (MO) recording using magnetic multifilm systems in recent years. In one of them, a $Pt_{84}Co_{16}$ film with in-plane easy axis has been coupled magnetically with the recording film of TbFeCo where the easy axis is perpendicular to the film.[1] A remarkable improvement in field sensitivity has been achieved with this structure, namely only one-tenth strength of the external field is enough for complete writing and erasing compared with the conventional MO disk with single magnetic film. This *capping effect* is very important in practical applications such as field modulation recording combined with the magnetic super resolution technology.

The purpose of this study is to clarify theoretically the properties of systems with magnetic double films which are exchange coupled.[2,3] The paper is organized as follows: Sec. II is devoted to the introduction of notations and basic formulation. The mechanism of the capping effect is clarified in Sec. III. Typical configurations and hysteresis loops are calculated in Sec. IV. In Sec. V, the capping effect is evaluated numerically and dynamic processes are discussed. The dependence of the capping effect on the thickness of the capping film is discussed in the remaining part of the paper. The phase transition between different alignments of magnetization as the thickness of the capping film is varied will be discussed in Sec. VI. As the critical point of the phase transition, the minimal thickness of capping film which shows the capping effect is also derived. The saturation of $H_{\rm cap}$ at large thickness is discussed in Sec. VII. Sec. VIII is devoted to summary and discussions.

II. FORMULATION

We study a magnetic system with exchange-coupled double films, where the easy axis is in-plane in film 1, the capping film of $Pt_{84}Co_{16}$, while it is perpendicular to the films in film 2, the recording film of TbFeCo. We take the z axis to be perpendicular to the films and the origin at the interface as shown in Fig. 1. The angle measured from the negative direction of the z axis is used to describe configurations of magnetization which is considered to be uniform in x and y directions. The thicknesses of film 1 and film 2 are denoted by a and b, respectively.

The total magnetic energy per unit area is expressed as[4]

$$\gamma=\int_0^a\left[A_1\left(\frac{d\varphi}{dz}\right)^2+(-K_1)\sin^2\varphi+M_{s1}H_{\rm ext}\cos\varphi\right]dz+\int_{-b}^0\left[A_2\left(\frac{d\varphi}{dz}\right)^2+K_2\sin^2\varphi+M_{s2}H_{\rm ext}\cos\varphi\right]dz\ , \quad (1)$$

where $A_{1(2)}$ and $K_{1(2)}$ stand for the stiffness constant and the absolute value of the anisotropy constant for the capping (recording) film, respectively. The anisotropy constants consist of a uniaxial anisotropy part and a demagnetization part, and are negative in film 1, while positive in film 2, as in the above total-energy expression. The direction of magnetization is supposed to be continuous at the interface between the films:[5,6]

$$\varphi|_{z=+0}=\varphi|_{z=-0}\ . \quad (2)$$

The external field $H_{\rm ext}$ is positive if it is applied in the

 ©1994 The American Physical Society

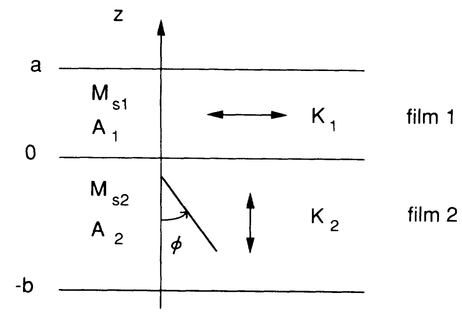

FIG. 1. Double-film system studied in this work.

TABLE I. Magnetic constants at room temperature and film dimensions.

	Capping film: 1	Recording film: 2
Material	$Pt_{84}Co_{16}$	TbFeCo
M_s [emu/cm^3]	200	90
A [erg/cm]	1.0×10^{-7}	2.0×10^{-7}
K [erg/cm^3]	0.25×10^{6}	2.0×10^{6}
Thickness [Å]	200	350

positive direction of the z axis.

Since the dimensionless quantity $b\sqrt{K_2/A_2}$, the thickness b of the recording film scaled by the characteristic length $\sqrt{A_2/K_2}$, is about ten for the system specified by Table I,[7] the thickness of the recording film may be taken as infinity as an approximation. We notice that this approximation is physically reasonable for any stable recording system and its applicability will be checked by numerical results. It is not difficult to see that in such an approximation the direction of magnetization at $z=-\infty$ is $\varphi=0$ or $\varphi=180°$.

By applying the variational method to energy (1) we obtain the following differential equations for the function $\varphi(z)$:

$$\begin{cases} K_1\dfrac{d\cos^2\varphi}{d\varphi}+M_{s1}H_{\rm ext}\dfrac{d\cos\varphi}{d\varphi}=2A_1\dfrac{d^2\varphi}{dz^2}, & 0\le z\le a, \\ K_2\dfrac{d\sin^2\varphi}{d\varphi}+M_{s2}H_{\rm ext}\dfrac{d\cos\varphi}{d\varphi}=2A_2\dfrac{d^2\varphi}{dz^2}, & z\le 0 \end{cases} \tag{3}$$

with three boundary conditions

$$\begin{cases} \left.\dfrac{d\varphi}{dz}\right|_{z=a}=\left.\dfrac{d\varphi}{dz}\right|_{z=-\infty}=0\,, \\ A_1\left.\dfrac{d\varphi}{dz}\right|_{z=+0}=A_2\left.\dfrac{d\varphi}{dz}\right|_{z=-0}\,. \end{cases} \tag{4}$$

The last condition is known as the Weierstrass-Erdmann law.[5,6]

In order to evaluate the external field required for complete recording in the present system and to lay some foundation for the discussion in the next section, let us consider the case of a positive external field $H_{\rm ext}$ and downward magnetization at the bottom surface of film 2, namely $\varphi|_{z=-\infty}=0$.

By multiplying $d\varphi/dz$ to the two equations in (3) and integrating them from $z=a$ and $z=-\infty$, respectively, we arrive at

$$\begin{cases} K_1(\cos^2\varphi-\cos^2\varphi_a)+M_{s1}H_{\rm ext}(\cos\varphi-\cos\varphi_a) \\ \qquad =A_1\left[\dfrac{d\varphi}{dz}\right]^2, \quad 0\le z\le a\,, \\ K_2\sin^2\varphi+M_{s2}H_{\rm ext}(\cos\varphi-1)=A_2\left[\dfrac{d\varphi}{dz}\right]^2, \quad z\le 0, \end{cases} \tag{5}$$

where the first and second conditions in (4) and $\varphi|_{z=-\infty}=0$ have been taken into account. The direction of magnetization at the top surface of film 1, φ_a, is introduced. As shown in Appendix A, the differential equations in (5) accompanied with (2) and the third condition in (4) can be reduced to a *single* nonlinear equation for φ_a:

$$\frac{\sqrt{A_2K_2/A_1K_1}}{\sqrt{1-k^2}\cos(\varphi_0/2)}\,\frac{\sqrt{1+\cos\varphi_0-h_2}}{\sqrt{h_1+2\cos\varphi_a}}=\frac{{\rm sn}[\hat{a},k]}{{\rm cn}[\hat{a},k]{\rm dn}[\hat{a},k]} \tag{6}$$

with Jacobian elliptic functions ${\rm sn}[\hat{a},k]$, ${\rm cn}[\hat{a},k]$, and ${\rm dn}[\hat{a},k]$ and

$$\begin{cases} \hat{a}=\dfrac{a}{2}\sqrt{K_1/A_1}\sqrt{(1+\cos\varphi_a)(1+\cos\varphi_a+h_1)}, \\ k^2=\dfrac{\tan^2(\varphi_a/2)(1-\cos\varphi_a-h_1)}{1+\cos\varphi_a+h_1}, \\ \tan\dfrac{\varphi_0}{2}=\tan\dfrac{\varphi_a}{2}\,\dfrac{{\rm cn}[\hat{a},k]}{{\rm dn}[\hat{a},k]}\,, \end{cases} \tag{7}$$

where $\varphi_0\equiv\varphi|_{z=+0}=\varphi|_{z=-0}$. The external field $H_{\rm ext}$ enters into the above equations through the parameters $h_{1(2)}=M_{s1(2)}H_{\rm ext}/K_{1(2)}$. Equation (6) is meaningless for $h_2>2$. This corresponds to external fields stronger than $2K_2/M_{s2}$. Under such strong external fields, the condition $\varphi|_{z=-\infty}=0$ is obviously broken. The region of external field studied in the present paper is smaller than $2K_2/M_{s2}\simeq 44$ kOe, and thus $h_2<2$.

The configuration of magnetization which minimizes energy (1) is derived as a by-product of Appendix A and is given explicitly in terms of φ_a or φ_0 as

$$\begin{cases} \tan\dfrac{\varphi}{2}=\tan\dfrac{\varphi_a}{2}\,\dfrac{{\rm cn}[\hat{a}-\hat{z},k]}{{\rm dn}[\hat{a}-\hat{z},k]}, \quad 0\le z\le a\,, \\ \tan\dfrac{\varphi}{2}=\dfrac{\sqrt{2/h_2-1}}{\cosh\{z\sqrt{K_2(1-h_2/2)/A_2}+\ln[\tan(\varphi_0/2)/(\sqrt{2/h_2-1}+\sqrt{2/h_2-\sec^2(\varphi_0/2)})]\}}, \quad z\le 0\,, \end{cases} \tag{8}$$

where $\hat{z}$ is defined in the same way as $\hat{a}$ in (7).

Similar equations for a negative external field can be derived in the same way, paying attention to the condition at the bottom surface of film 2.

III. ORIGIN OF THE CAPPING EFFECT

Using the theoretical framework derived in the last section, we are now ready to clarify the role of the exchange coupling between the films. Without the capping film, the direction of magnetization at the top surface of film 2 should be subjected to

$$K_2\sin^2\varphi - 2M_{s2}H_{\text{ext}}\sin^2(\varphi/2) = 0 , \tag{9}$$

from the second equation in (5), since $d\varphi/dz|_{z=-0}=0$ in this case. However, for the magnetic double-film system with exchange coupling we should have, instead of the above relation,

$$K_2\sin^2\varphi - 2M_{s2}H_{\text{ext}}\sin^2(\varphi/2) = E_{\text{ex}} \tag{10}$$

with $E_{\text{ex}} = A_2(d\varphi/dz)^2$. Therefore, the term E_{ex} is a result of the exchange coupling between the magnetic films. Noting E_{ex} is positive as well as the external field in the above equation, we find that the effect of the exchange coupling is to enhance the external field. This is the origin of the capping effect observed in experiments.

In order to give quantitative estimation, we define the field enhancement by regarding the exchange energy E_{ex} as an effective Zeeman term:

$$H_{\text{cap}} = \frac{E_{\text{ex}}}{M_{s2}\cos\varphi_0} \tag{11}$$

with the direction of magnetization at the interface φ_0. The field H_{cap} is induced by the exchange coupling and determined by the magnetic constants A's and K's in both of the films and the thickness of the capping film as well as the external field.

We notice that the field H_{cap} is meaningful when the temperature is quite far from the compensation temperature of the ferrimagnetic material in the recording film. Fictitious divergence of H_{cap} occurs when the external field is so strong so that $\varphi_0 \simeq 90°$. In these cases it is better for us to discuss the exchange-coupling energy E_{ex} itself. Most of the following arguments work for the quantity E_{ex}.

From the second equation in (5) we have the following analytic expression for H_{cap}:

$$H_{\text{cap}} = \frac{\sin^2\varphi_0}{\cos\varphi_0}\left[1 - \frac{h_2}{2\cos^2(\varphi_0/2)}\right]\frac{K_2}{M_{s2}} , \tag{12}$$

where φ_0 is determined by (6) and (7). This expression of H_{cap} is also applied to other regions in the recording film, provided that the corresponding direction of magnetization $\varphi(z)$ is used.

IV. TYPICAL CONFIGURATIONS, HYSTERESIS LOOPS, AND COERCIVE FORCE

The configuration of magnetization is evaluated by (8) and is displayed in Fig. 2 for the case of $H_{\text{ext}} = 50$ Oe.

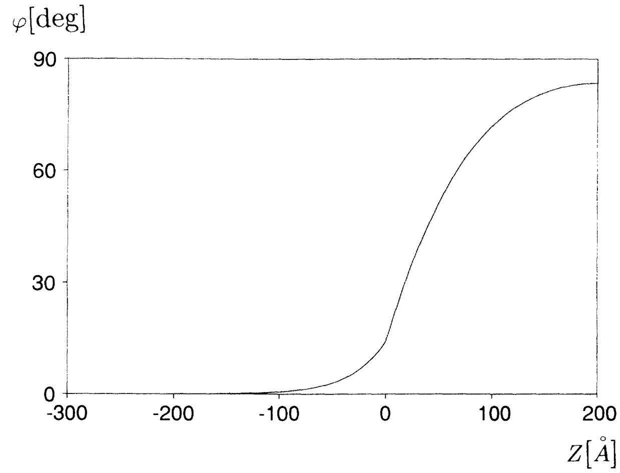

FIG. 2. Configuration under $H_{\text{ext}} = 50$ Oe. Positive (negative) coordinates denote the region of the capping (recording) film.

The direction of magnetization at the interface is $\varphi_0 \simeq 14.2°$, while that at the top surface is $\varphi_a \simeq 83.5°$. $\varphi(z)$ drops exponentially inside the recording film and becomes almost zero at 200 Å from the interface. This feature justifies our approximation that $b=\infty$. For comparison, the configuration under a strong external field of $H_{\text{ext}} = 7500$ Oe is shown in Fig. 3. It is found that under such a strong external field the direction of magnetization at the top surface of the system is almost aligned with the external field.

By varying the external field continuously we have obtained hysteresis loops for the magnetization at various positions. The hysteresis loop for φ_a, the direction of magnetization at the top surface, shown in Fig. 4 is much thinner than the one for φ_0, the direction of magnetization at the interface, shown in Fig. 5. This fact suggests that the magnetization in the capping film respond to the external field quickly and then pull the magnetization in the recording film through the exchange coupling, as revealed in Sec. III and discussed from the experimental

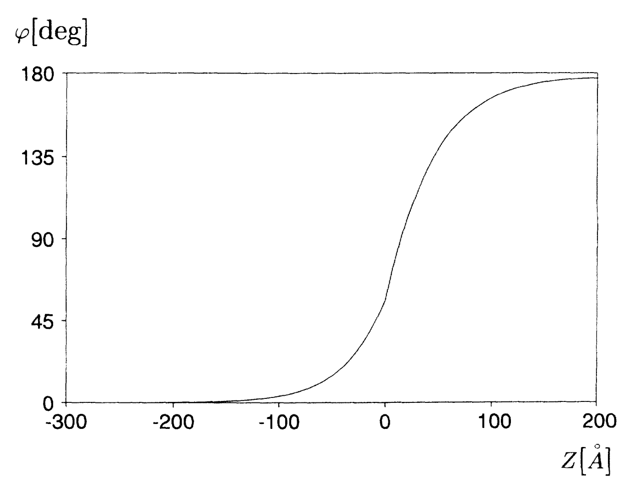

FIG. 3. The same with Fig. 2 except for $H_{\text{ext}} = 7500$ Oe.

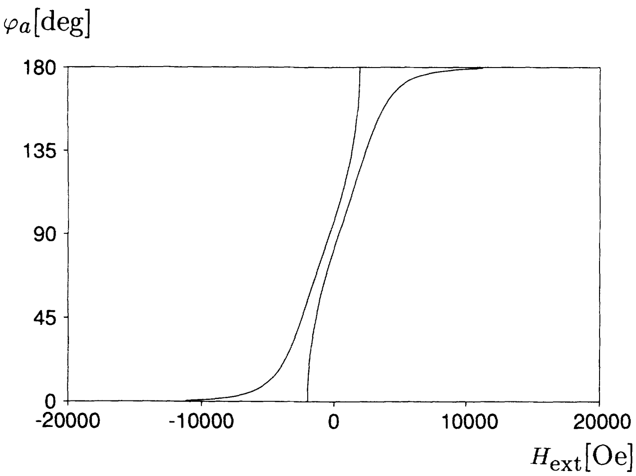

FIG. 4. Hysteresis loop for the magnetization at the top surface of the double-film system.

side qualitatively.[1]

There are two vertical parts at $H_{\rm ext} \simeq \pm 11$ kOe in the hysteresis loop for φ_0 in Fig. 5. This value of the external field may be considered as the coercivity H_c for the present magnetic double-film system. The coercive force of the single recording film should be $2K_2/M_{s2} \simeq 44$ kOe in the present model. Thus, we have found that the presence of nonuniformity in the system, introduced by the capping film with in-plane easy axis in the present case, reduces the coercive force significantly from that of a uniform system. This result is consistent qualitatively with experimental observations. Nevertheless, we notice that the coercive force measured by experiments for the present magnetic double-film system is about 3 kOe.[7] Therefore, in order to understand the capping effect quantitatively, fine structures in the films have to be treated. This is not our present concern.

The minimal and maximal values of φ_0 assumed at the endpoints of the vertical part for positive external field are 90° and 180°, respectively. Since φ_0 is positive and

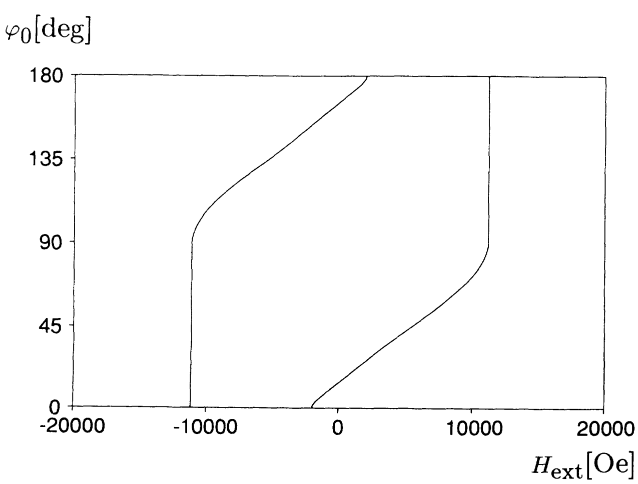

FIG. 5. Hysteresis loop for the magnetization at the interface of the double-film system. The coercivity H_c is about 11 kOe.

less than 90° under the external field $0 \le H_{\rm ext} < H_c$, we find that $H_{\rm cap}$ defined by (11) enhances the external field in this region. For $H_{\rm ext} > H_c$ the condition $\varphi|_{z=-\infty}=0$ is broken and $\varphi|_{z=-\infty}=180°$ should be adopted and it is not difficult to see that $H_{\rm cap}=0$ in this case. The same arguments apply to the left branch of the hysteresis loop in Fig. 5.

We have found that one obtains hysteresis loops for φ_0 with different shapes and different values of the coercive force H_c as the thickness of the capping film is varied. At infinite thickness, the coercive force is about 8 kOe and the hysteresis loop is similar to the one for $a=200$ Å as shown in Fig. 5. However, when the thickness is reduced, the hysteresis loop gets more rectangular, becoming exact rectangle when the thickness becomes less than a certain value $a_{\rm min}$. The coercive force in this case is equal to $2K_2/M_{s2}$. The vanishing of the capping effect for small capping film thickness will be discussed fully in Sec. VI.

As shown in Appendix B, the coercive force of the magnetic double-film system with sufficiently thick capping film can be derived analytically:

$$H_c = \frac{A_1K_1 + A_2K_2}{A_1M_{s1} + A_2M_{s2}} . \tag{13}$$

For a double-film system with same magnitudes of magnetic constants in the two films, we have $H_c = K_2/M_{s2}$ from the above relation, which is only half of that of the single recording film, $2K_2/M_{s2}$. Relation (13) can be rewritten as

$$H_c = \frac{K_2}{M_{s2}} \frac{1 + A_1K_1/A_2K_2}{1 + A_1M_{s1}/A_2M_{s2}} . \tag{14}$$

It is then apparent that a capping film satisfying

$$\frac{A_1K_1}{A_2K_2} < 1 + 2\frac{A_1M_{s1}}{A_2M_{s2}} \tag{15}$$

will result in a coercive force of the double-film system smaller than $2K_2/M_{s2}$. The above inequality is satisfied in the system where magnetic material with smaller Néel-wall energy is adopted as the capping film, namely $\sqrt{A_1K_1} < \sqrt{A_2K_2}$, no matter how large the magnetizations are.

V. VALUE OF THE FIELD ENHANCEMENT $H_{\rm cap}$

In the present section, the field enhancement $H_{\rm cap}$ is investigated quantitatively. The external field is set at $H_{\rm ext} = 50$ Oe, which is found experimentally to be the minimal external field for complete recording in the present magnetic double-film system.[1]

The field enhancement at the interface is evaluated as $H_{\rm cap} \simeq 1337$ Oe from (12). This value may be interpreted as follows: Under the uniform external field of $H_{\rm ext}=50$ Oe, the magnetization in the recording film experiences an effective field of $H_{\rm eff} = H_{\rm ext} + H_{\rm cap} \simeq 1387$ Oe near the interface.

The field enhancement assumes its maximum at the interface and drops very quickly inside the recording film as seen in Fig. 6. Therefore, nucleations of magnetization reversal take place certainly at the interface. When the external field is increased to the coercive force H_c, the direction of magnetization at the interface changes abruptly from $\varphi=90°$ to $\varphi=180°$ as suggested by the hysteresis loop in Fig. 5. The locus where the maximal field enhancement is assumed, shifts inside the recording film. This in turn results in magnetization reversal at a deeper part of the recording film. In other words, nucleation at the interface is followed by a movement of magnetic wall. This mechanism of the magnetization reversal may be called a *domino phenomenon triggered by accidental nucleation.*

VI. DEPENDENCE OF H_{cap} ON THICKNESS OF THE CAPPING FILM

The dependence on thickness of the capping film is another important aspect of the capping effect in magnetic double-film systems. We have found a strong nonlinear behavior of the field enhancement H_{cap}. First, there is a minimal thickness of the capping film needed to show the capping effect. Secondly, the critical behavior in the vicinity of the minimal thickness is described by

$$H_{cap} \sim a - a_{min}, \quad a \geq a_{min} . \tag{16}$$

Thirdly, the field enhancement H_{cap} saturates at large thickness. The detailed behavior of H_{cap} as a function of the thickness of the capping film under $H_{ext}=50$ Oe is shown in Fig. 7. The critical thickness is $a_{min} \simeq 82$ Å.

A similar behavior was found by Wakabayashi, Notarys, and Suzuki for the direction of magnetization at the top surface by numerical calculations with a discrete model.[9] However, in order to get the full picture of this phenomenon, namely to obtain the explicit dependence of the critical thickness on the magnetic constants of the two films, it is essential to clarify theoretically the mechanism of the above phase transition and to study the

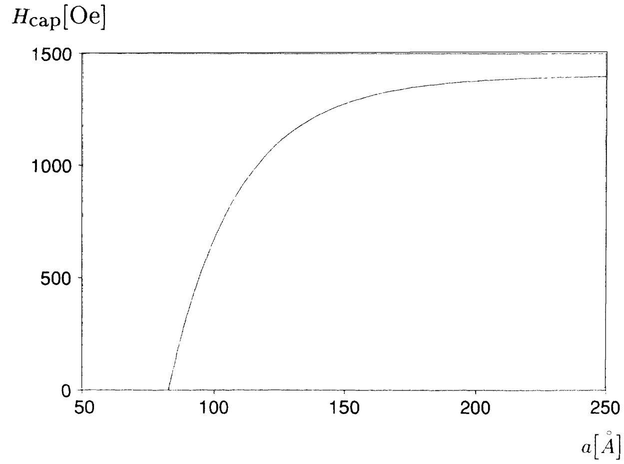

FIG. 7. Dependence of the field enhancement on the thickness of the capping film under $H_{ext}=50$ Oe. The minimal thickness of the capping film that shows capping effect is $a_{min} \simeq 82$ Å. The saturation value of the field enhancement H_{cap} is about 1.4 kOe.

minimal thickness, critical behavior and critical tangent analytically. We notice that expressions in (6) and (7) are a single nonlinear equation for the variable φ_a. This feature of the present approach makes the investigation of properties of magnetic double-film systems much easier.

For the sake of simplicity, let us first consider the case of null field. As shown in Appendix C, the equation for φ_a is simplified to

$$\frac{\sqrt{A_2K_2}}{\sqrt{A_1K_1}} = \frac{\mathrm{sn}[a\sqrt{K_1/A_1}, \sin\varphi_a]}{\mathrm{cn}[a\sqrt{K_1/A_1}, \sin\varphi_a]} \cos\varphi_a . \tag{17}$$

The right-hand side of the above equation

$$y(\varphi;a) = \frac{\mathrm{sn}[a\sqrt{K_1/A_1}, \sin\varphi]}{\mathrm{cn}[a\sqrt{K_1/A_1}, \sin\varphi]} \cos\varphi \tag{18}$$

shows such dependence on a and φ as sketched in Fig. 8.

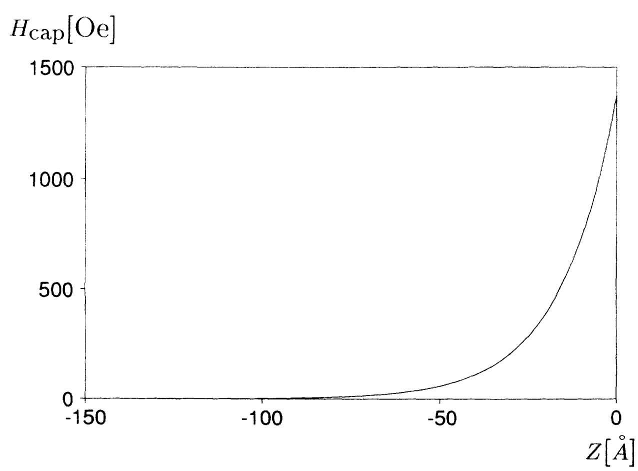

FIG. 6. Profile of field enhancement in the recording film (denoted by negative coordinates) under $H_{ext}=50$ Oe. The maximal field enhancement is about 1.3 kOe and is assumed at the interface ($z=0$).

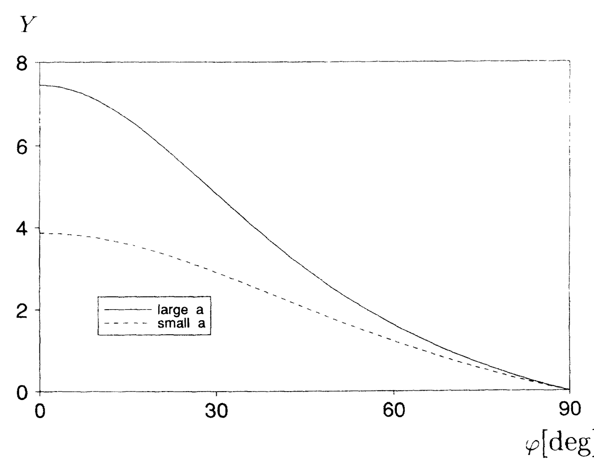

FIG. 8. Dependence of y of (18) on a and φ.

The function $y(\varphi;a)$ increases uniformly as a increases. Therefore, for a value of $\sqrt{A_2K_2/A_1K_1}$ determined by the temperature of the system, there is no cross between the horizontal line $y=\sqrt{A_2K_2/A_1K_1}$ and the curve $y=y(\varphi;a)$, and thus no solution to (17), if a is not sufficiently large. Since the function $y(\varphi;a)$ assumes its maximum at $\varphi=0$ as is seen in Fig. 8, we can determine the minimal thickness for the existence of solution of (17) by setting $\varphi_a=0$. Noting $\mathrm{sn}[x,0]=\sin x$ and $\mathrm{cn}[x,0]=\cos x$, we arrive at

$$a_{\min}=\sqrt{A_1/K_1}\,\tan^{-1}\frac{\sqrt{A_2K_2}}{\sqrt{A_1K_1}}\ , \tag{19}$$

for the minimal thickness at null field. The physical meaning of the above expression is very clear: The minimal thickness of the capping film in the present magnetic double-film system is determined by the arctangent of the ratio between the energies stocked in Néel-type walls in bulk systems of materials of the recording film and of the capping film beside a prefactor proportional to the thickness of Néel-type wall in material of the capping film.

When the thickness is less than the above critical value, there is no solution to (17), and Eq. (5) has to take the trivial solution $\varphi(z)=0$. It is easy to see that the uniform function $\varphi(z)=0$ is always a solution of (5). Therefore, the phase transition such as that shown in Fig. 7 is a bifurcation of (5), and the minimal thickness (19) is the bifurcation point. Since $H_{\mathrm{cap}}=0$ for the trivial solution $\varphi(z)=0$, $a_{\min}$ in (19) is the minimal thickness of the capping film that exhibits the capping effect in magnetic double-film systems.

The dependence of H_{cap} on the thickness a when it is slightly above the minimal value can also be derived analytically. Since the solution φ_a of (17) is small in the critical region, the following expansions of Jacobian elliptic functions up to the second order of $k=\sin\varphi_a$ are sufficient for analysis in the vicinity of the critical point:

$$\begin{cases}\mathrm{sn}[x,k]\simeq \sin x-\frac{1}{4}\cos x\,(x-\frac{1}{2}\sin 2x)k^2\ ,\\ \mathrm{cn}[x,k]\simeq \cos x+\frac{1}{4}\sin x\,(x-\frac{1}{2}\sin 2x)k^2\ .\end{cases} \tag{20}$$

Equation (17) is simplified up to the second order of φ_a as

$$\frac{\sqrt{A_2K_2}}{\sqrt{A_1K_1}}=\tan\tilde{a}-[\tfrac{1}{4}(\tilde{a}_{\min}-\tfrac{1}{2}\sin 2\tilde{a}_{\min})\sec^2\tilde{a}_{\min}+\tfrac{1}{2}\tan\tilde{a}_{\min}]\sin\varphi_a^2\ , \tag{21}$$

where $\tilde{a}=a\sqrt{K_1/A_1}$ and $\tilde{a}_{\min}=a_{\min}\sqrt{K_1/A_1}$. The solution of (17) in the vicinity of the critical thickness is then

$$\sin\varphi_a^2=\frac{8(\tan\tilde{a}-\tan\tilde{a}_{\min})}{(2\tilde{a}_{\min}-\sin 2\tilde{a}_{\min})\sec^2\tilde{a}_{\min}+4\tan\tilde{a}_{\min}}\ , \tag{22}$$

where (19) has been used. Since the difference between φ_a and φ_0 contributes only in higher orders as is seen from (7), we arrive at the critical behavior of H_{cap} by including the above solution into (12) and setting $h_2=0$:

$$H_{\mathrm{cap}}\simeq\hat{H}_{\mathrm{cap}}(a-a_{\min})\sqrt{K_1/A_1},\quad a\ge a_{\min} \tag{23}$$

with

$$\hat{H}_{\mathrm{cap}}=\frac{4K_2/M_{s2}}{(1+A_2K_2/A_1K_1)\tan^{-1}\sqrt{A_2K_2/A_1K_1}+\sqrt{A_2K_2/A_1K_1}}\ . \tag{24}$$

Similar arguments can be performed for finite external fields. The resulting expression for the minimal thickness is derived from (6) as

$$a_{\min}=\frac{\sqrt{A_1/K_1}}{\sqrt{1+h_1/2}}\tan^{-1}\frac{\sqrt{A_2K_2(1-h_2/2)}}{\sqrt{A_1K_1(1+h_1/2)}}\ . \tag{25}$$

This analytic result relates the stiffness constants, anisotropy constants, saturation magnetizations, and the external field to the minimal thickness of the capping layer that shows the capping effect. The external field reduces the minimal thickness through the parameters h_1 and h_2. The critical behavior under a finite external field is of the same form given in (23).

VII. SATURATION VALUE OF H_{cap}

Saturation of the field enhancement at large thickness of the capping film is another interesting aspect of the capping effect. It is of practical importance as well since it states that there is a maximal field enhancement for the given two materials. The saturation field enhancement is $H_{\mathrm{cap}}\simeq 1397$ Oe for the present system under $H_{\mathrm{ext}}=50$ Oe as shown in Fig. 7.

Since H_{cap} saturates completely at infinite thickness of the capping film, we have derived in Appendix D the following equation for φ_0 in a system with two exchange-coupled bulk materials:

$$\frac{\sqrt{A_2K_2}}{\sqrt{A_1K_1}}=\frac{(\cos\varphi_0+h_1/2)\sqrt{1+\cos\varphi_0}}{\sin\varphi_0\sqrt{1+\cos\varphi_0-h_2}}\ . \tag{26}$$

Employing the solution of the above equation in (12), an expression for the saturation of the field enhancement H_{cap}^s is obtained. At null field, the solution of (26) is $\varphi_0=\cot^{-1}\sqrt{A_2K_2/A_1K_1}$ and thus the saturation field enhancement is given as

$$H_{\mathrm{cap}}^s=\frac{K_2}{M_{s2}}\frac{\sin^2\varphi_0}{\cos\varphi_0}=\frac{K_2}{M_{s2}}\frac{\sqrt{A_1K_1}}{\sqrt{A_2K_2}}\frac{\sqrt{A_1K_1}}{\sqrt{A_1K_1+A_2K_2}}\ . \tag{27}$$

With the constants in Table I, it is evaluated as

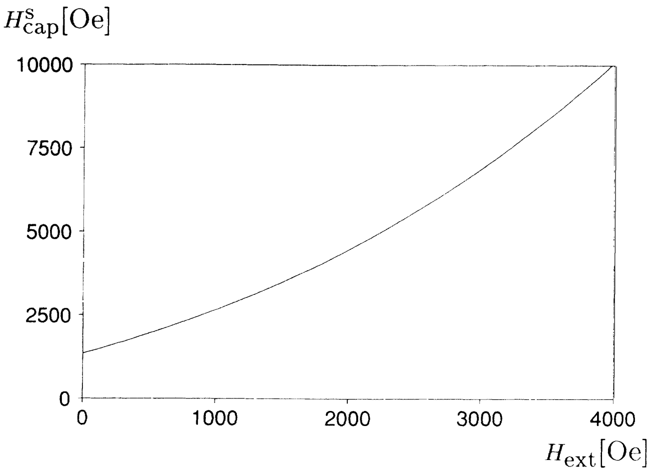

FIG. 9. Saturated value of the field enhancement vs the strength of the external field.

$H^s_{cap} \simeq 1347$ Oe. As shown in Fig. 9, H^s_{cap} depends on the external field almost linearly.

VIII. SUMMARY

We have studied the effect of the exchange coupling between the recording film and the capping film by imposing the continuity of the directions of magnetization at the interface and using the variational method to minimize the summations of exchange energy, anisotropy energy, and Zeeman energy. We have found that the nonuniformity introduced by the capping film with inplane anisotropy axis reduces significantly the hardness of the system. This result is qualitatively consistent with experimental observations. The coercivity for the magnetic double-film system is derived analytically.

We have defined the field enhancement H_{cap} by regarding the exchange energy at the interface as an effective Zeeman energy. Since it is found that H_{cap} is localized at the interface, the dynamic process of magnetization reversal in the magnetic double-film system is almost certainly a *domino* phenomenon triggered by accidental nucleation at the interface.

Concerning the dependence of H_{cap} on the thickness of the capping film, we have derived an analytic expression for the minimal thickness a_{min} of the capping film that shows the capping effect, in terms of the stiffness constants, anisotropy constants, saturation magnetizations, and external field. The mechanism responsible for the phase transition between different alignments of magnetization has been clarified and the critical behavior of H_{cap} in the vicinity of a_{min} is derived. We have also studied the saturation of H_{cap} at large thickness. These features are important as well in design of magnetic multifilm systems.

Several simplifications have been made in the present approach: First, the saturation magnetizations, stiffness constants, and anisotropy constants are assumed to be uniform in each film and to change abruptly at the interface. Secondly, the direction of magnetization is assumed to be continuous at the interface. These two treatments are usually adopted in continuum models. Thirdly, the configuration of magnetization is taken to be uniform in directions parallel to the films. This approximation should be adequate since the phenomena discussed in the present paper occur on a scale of order of 100 Å, while typical recording marks in MO disks are of order of 1 μm. It is reasonable to assume that the magnetic properties are uniform in the recording mark. Fourthly, the recording film is approximated as one of infinite thickness. This approximation is sufficient for stable recording disks and its applicability is verified by the present numerical results.

The temperature dependence of the capping effect is an important aspect to be clarified, since in MO recording a laser spot is used and the temperature is increased locally. A phase transition is expected as the temperature is varied, similar to the one discussed in the present paper. Interesting phenomena may also be observed when the temperature of the system crosses the compensation points and/or near the Curie points of the films. It may be possible that the present definition of H_{cap} by the total magnetization M_{s2} fails when the temperature gets nearer to the compensation temperature of the recording film. In this case, sublattice magnetizations should be considered. Detailed studies are now in progress and will be reported in the near future.

The effects of thermal fluctuations on the phase transitions in the present system of a magnetic thin layer coupled to a magnetic semi-infinite bulk, should be studied by the modern theory of phase transitions and critical phenomena. Although the established works for semi-infinite systems[10] will certainly shed light to the present system, several new aspects should be clarified. The role played by the thickness of the thin layer in the phase transition may be the most important issue to be addressed.[11]

The present analytic study of the magnetic nonuniform system may also shed light on the mechanism of the coercivity in amorphous alloys. A detailed discussion about this aspect will be reported elsewhere.

ACKNOWLEDGMENTS

We are indebted to Dr. N. Ohta, Dr. T. Yorozu, and Mr. S. Ohnuki in Hitachi Maxell Co. for drawing our attention to the present problem, stimulating discussions, and providing us with experimental data before publication. We are grateful to Dr. T. Yorozu for helpful comments on the manuscript. Thanks are due to Professor M. van Schilfgaarde for valuable advice about English expressions. Numerical calculations have been performed on an IBM 9370 at the Institute for Materials Research at Tohoku University and an IBM 3090 at Education Center for Information Processing, Tohoku University. The authors are grateful for the Partnership program with IBM Japan for the implementation of computer resources and also for the technical help in computation from Y. Akiyama and M. Ikeda. Dr. Hu is supported in part by the Scientific Research Fund of the Ministry of Education, Science and Culture of Japan and in part by a grant from Iketani Science and Technology Foundation.

APPENDIX A: DERIVATION OF (6)

In this appendix, we reduce Eq. (5) to a single nonlinear equation. This process makes the behavior of the system much more transparent. The first equation in (5) can be integrated using (2.580.2) of Ref. 8 as:

$$z=a-\sqrt{A_1/K_1}\int_{\varphi}^{\varphi_a}\frac{d\varphi}{\sqrt{\cos^2\varphi-\cos^2\varphi_a+h_1(\cos\varphi-\cos\varphi_a)}}$$
$$=a-2\sqrt{A_1/K_1}\int_{\tan(\varphi/2)}^{\tan(\varphi_a/2)}dx\left[\frac{[(1+\cos\varphi_a)(-1+\cos\varphi_a+h_1)]^{-1}}{[\tan^2(\varphi_a/2)-x^2][x^2+(1+\cos\varphi_a+h_1)/(-1+\cos\varphi_a+h_1)]}\right]^{1/2}. \tag{A1}$$

For weak external fields, where $-1+\cos\varphi_a+h_1<0$, the above integral can be evaluated using (3.125.8) of Ref. 8 as

$$z=a-2\sqrt{A_1/K_1}\int_{\tan(\varphi/2)}^{\tan(\varphi_a/2)}dx\frac{\sqrt{[(1+\cos\varphi_a)(1-\cos\varphi_a-h_1)]^{-1}}}{\sqrt{[\tan^2(\varphi_a/2)-x^2][(1+\cos\varphi_a+h_1)/(1-\cos\varphi_a-h_1)-x^2]}}$$
$$=a-\frac{2\sqrt{A_1/K_1}}{\sqrt{(1+\cos\varphi_a)(1+\cos\varphi_a+h_1)}}\left\{F\left[\frac{\pi}{2},k\right]-F\left[\sin^{-1}\left[\frac{\tan(\varphi/2)}{\tan(\varphi_a/2)}\right],k\right]\right\}, \tag{A2}$$

where $F[x,k]$ is the elliptic integral of the first kind and k is defined in the second relation in (7). Thus, we arrive at the third relation in (7)

$$\tan\frac{\varphi_0}{2}=\tan\frac{\varphi_a}{2}\mathrm{sn}\left[F\left[\frac{\pi}{2},k\right]-\hat{a},k\right]=\tan\frac{\varphi_a}{2}\frac{\mathrm{cn}[\hat{a},k]}{\mathrm{dn}[\hat{a},k]} \tag{A3}$$

with $\hat{a}$ defined by the first relation in (7).

The quantity appears on the left-hand side of the third condition in (4) is evaluated as

$$A_1\frac{d\varphi}{dz}\Big|_{z=+0}=\cos^2\frac{\varphi_0}{2}\sqrt{A_1K_1}\sqrt{(1+\cos\varphi_a)(1-\cos\varphi_a-h_1)}$$
$$\times\left[\left[\tan^2\frac{\varphi_a}{2}-\tan^2\frac{\varphi_0}{2}\right]\left[\frac{1+\cos\varphi_a+h_1}{1-\cos\varphi_a-h_1}-\tan^2\frac{\varphi_0}{2}\right]\right]^{1/2}. \tag{A4}$$

The second equation in (5) is also integrated using (2.580.2) of Ref. 8 as

$$z=\frac{\sqrt{A_2/K_2}}{\sqrt{1-h_2/2}}\ln\frac{\tan(\varphi/2)[\sqrt{2/h_2-1}+\sqrt{2/h_2-1-\tan^2(\varphi_0/2)}]}{\tan(\varphi_0/2)[\sqrt{2/h_2-1}+\sqrt{2/h_2-1-\tan^2(\varphi/2)}]}. \tag{A5}$$

The quantity appears on the right-hand side of the third condition in (4) is evaluated as

$$A_2\frac{d\varphi}{dz}\Big|_{z=-0}=\sin\varphi_0\sqrt{A_2K_2}\left[1-\sec^2\frac{\varphi_0}{2}\frac{h_2}{2}\right]^{1/2}. \tag{A6}$$

Equation (6) is then derived with some algebra, employing the quantities in (A4) and (A6) in the third condition in (4).

For strong external fields, where $-1+\cos\varphi_a+h_1>0$, Eqs. (A3) and (A4) are replaced by

$$\tan\frac{\varphi_0}{2}=\tan\frac{\varphi_a}{2}\mathrm{cn}[\hat{a},k] \tag{A7}$$

with

$$\hat{a}=a\sqrt{K_1/A_1}\sqrt{\cos\varphi_a+h_1/2},\quad k^2=\frac{\sin^2(\varphi_a/2)(-1+\cos\varphi_a+h_1)}{2\cos\varphi_a+h_1}, \tag{A8}$$

and

$$A_1\frac{d\varphi}{dz}\Big|_{z=+0}=\cos\frac{\varphi_0}{2}\sqrt{A_1K_1}\sqrt{(1+\cos\varphi_a)(-1+\cos\varphi_a+h_1)}$$
$$\times\left[\left[\tan^2\frac{\varphi_a}{2}-\tan^2\frac{\varphi_0}{2}\right]\left[\frac{1+\cos\varphi_a+h_1}{-1+\cos\varphi_a+h_1}+\tan^2\frac{\varphi_0}{2}\right]\right]^{1/2}. \tag{A9}$$

Thus, we have, instead of (6),

$$\frac{\sqrt{A_2K_2/A_1K_1}}{\cos(\varphi_0/2)}\frac{\sqrt{1+\cos\varphi_0-h_2}}{\sqrt{h_1+2\cos\varphi_a}}=\frac{\mathrm{sn}[\hat{a},k]\mathrm{dn}[\hat{a},k]}{\mathrm{cn}[\hat{a},k]} .$$

APPENDIX B: DERIVATION OF (13)

Since $\varphi_a=180°$ and $\varphi_0=90°$ at $H_{\rm ext}=H_c$, we have from (A9) and (A6)

$$A_1\frac{d\varphi}{dz}\bigg|_{z=+0}=\sqrt{A_1K_1}\sqrt{-1+h_1} \tag{B1}$$

and

$$A_2\frac{d\varphi}{dz}\bigg|_{z=-0}=\sqrt{A_2K_2}\sqrt{1-h_2} . \tag{B2}$$

The third condition in (4) then reads as

$$\sqrt{A_2K_2/A_1K_1}=\sqrt{(h_1-1)/(1-h_2)} , \tag{B3}$$

and leads to (13).

APPENDIX C: DERIVATION OF (17)

We derive the desired equation (17) directly from the following differential equations:

$$\begin{cases} K_1(\cos^2\varphi-\cos^2\varphi_a)=A_1\left[\dfrac{d\varphi}{dz}\right]^2, \quad 0\le z\le a , \\ K_2\sin^2\varphi=A_2\left[\dfrac{d\varphi}{dz}\right]^2, \quad z\le 0 , \end{cases} \tag{C1}$$

which are obtained from (5) setting $H_{\rm ext}=0$. The first equation can be integrated as

$$\begin{aligned} z&=a-\sqrt{A_1/K_1}\int_\varphi^{\varphi_a}\frac{d\varphi}{\sqrt{\cos^2\varphi-\cos^2\varphi_a}} \\ &=a-\sqrt{A_1/K_1}\left\{F\left[\frac{\pi}{2},\sin\varphi_a\right]\right. \\ &\qquad\left.-F\left[\sin^{-1}\left[\frac{\sin\varphi}{\sin\varphi_a}\right],\sin\varphi_a\right]\right\} , \end{aligned} \tag{C2}$$

where (2.615.1) of Ref. 8 has been used.

Thus, we have

$$\sin\varphi_0=\sin\varphi_a\frac{\mathrm{cn}[\tilde{a},\sin\varphi_a]}{\mathrm{dn}[\tilde{a},\sin\varphi_a]} , \tag{C3}$$

where $\tilde{a}=a\sqrt{K_1/A_1}$. Since

$$\begin{aligned} A_1\frac{d\varphi}{dz}\bigg|_{z=+0}&=\sqrt{A_1K_1}\sqrt{\cos^2\varphi_0-\cos^2\varphi_a} \\ &=\sqrt{A_1K_1}\sin\varphi_a\cos\varphi_a\frac{\mathrm{sn}[\tilde{a},\sin\varphi_a]}{\mathrm{dn}[\tilde{a},\sin\varphi_a]} \end{aligned} \tag{C4}$$

and

$$A_2\frac{d\varphi}{dz}\bigg|_{z=-0}=\sqrt{A_2K_2}\sin\varphi_a\frac{\mathrm{cn}[\tilde{a},\sin\varphi_a]}{\mathrm{dn}[\tilde{a},\sin\varphi_a]} \tag{C5}$$

from (C1) and (C3), we arrive finally at (17).

APPENDIX D: DERIVATION OF (26)

At the limit $a=\infty$, φ_a should satisfy $\cos\varphi_a=-h_1/2$, which minimizes the sum of the anisotropy energy and the Zeeman energy in the capping film. The quantity on the left-hand side of the third condition in (4) is then evaluated as

$$A_1\frac{d\varphi}{dz}\bigg|_{z=+0}=\sqrt{A_1K_1}(\cos\varphi_0+h_2/2) . \tag{D1}$$

With this relation and (A6), the third condition in (4) leads to (26).

[1]S. Ohnuki, K. Shimazaki, N. Ohta, and H. Fujiwara, J. Magn. Soc. Jpn., **15**, Suppl. S1, 399 (1991); S. Ohnuki, S. Shimazaki, and N. Ohta (unpublished).

[2]X. Hu, T. Yorozu, Y. Kawazoe, S. Ohnuki, and N. Ohta, Proceedings of INTERMAG'93, April, 1993, Stockholm, Sweden [IEEE Trans. Magn. (to be published)].

[3]Y. Kawazoe, X. Hu, and S. Honma, in *Magnetic Ultrathin Films: Multilayers and Surface/Interfaces and Characterization,* edited by B. T. Janker *et al.*, MRS Symposia Proceedings No. 313 (Materials Research Society, Pittsburgh, 1993), p. 513.

[4]W. F. Brown, Jr., *Micromagnetics* (Interscience, New York, 1963).

[5]I. M. Gelfand and S. V. Fomin, *Calculus of Variations,* translated by R. A. Silverman (Princeton-Hall, Englewood Cliffs, NJ, 1963).

[6]M. Kaneko, K. Aratani, Y. Mutoh, A. Nakaoki, K. Watanabe, and H. Makino, Jpn. J. Appl. Phys., Suppl. **28-3**, 927 (1989).

[7]N. Ohta, T. Yorozu, and S. Ohnuki (private communication).

[8]I. S. Gradshteyn and I. M. Ryzhik, *Tables of Integrals, Series, and Products* (Academic, New York, 1980).

[9]H. Wakabayashi, H. Notarys, and T. Suzuki, J. Magn Soc. Jpn., **15**, Suppl. S1, 87 (1991).

[10]See, for example, the review article by K. Binder, in *Phase Transitions and Critical Phenomena,* edited by C. Domb and J. L. Lebowitz (Academic, New York, 1983), and references therein.

[11]X. Hu *et al.* (unpublished).